Research Article

SOHAG JOURNAL OF SCIENCES

https://doi.org/10.21608/sjsci.2023.201834.1073

Gold Nanoparticles Induction Using Kombucha SCOBY Disc

M. Bassam Aboul-Nasr, Sabah S. Mohamed, and M. Seif-Elnasr Mohamed*

Botany and Microbiology Department, Faculty of Science, Sohag University, Sohag 82524, Egypt.
**Email: muhamedsci@yahoo.com*

Received: 10th May 2023, **Revised:** 3rd July 2023, **Accepted:** 3rd July 2023
Published online: 10th July 2023

Abstract: SCOBY disc is a unique structure of bacteria and fungi. It was known in the mid-Seventies in Egypt as "Tea fish." To the author's knowledge, no reports since then were published to use them in producing nanoparticles worldwide. The addition of 1mM of ($HAuCl_4.3H_2O$) solution into the cell-free extract (CFE) of SCOBY disc grew on black tea medium, resulted in gold nanoparticles AuNPs at 25ºC ($Au^{3+} \rightarrow Au^0$) momentarily. The surface plasmon resonance peaks of the gold colloidal solution produced showed an absorption peak at 530 nm. (TEM) exhibited AuNPs in spherical and triangle shapes (12 to 35 nm). X-ray diffraction reflected four distinct peaks at 2θ = 38.1°, 44.3°, 64.5°, and 77.7°. All four peaks corresponded to standard Bragg reflections (111), (200), (220), and (311) of face center cubic. (FTIR) analysis showed the presence of two amide groups in 1721 & 1033 respectively, which appeared to be responsible for the stability of gold nanoparticles. The mean particle size and polydispersity index (PDI) of AuNPs induced by SCOBY were 61.23 ± 0.416 with a negative charge -10.2 ± 1.73 mV that cause electrostatic repulsion among the nanoparticles and good colloidal stability. Moreover, the effect of AuNPs on inducing apoptosis in liver cancer cells HepG2. 3-(4,5-dimethylthiazol-2-yl)-2-5-diphenyltetrazolium bromide (MTT) assay showed that AuNPs produced had selective toxic effects to HepG2 cells with IC-50 value 176 µM/mL compared to control cells. These results suggested the use of those green synthesized AuNPs in cancer treatment and further studies are recommended.
Keywords: SCOBY, Kombucha, AuNPs, Cytotoxicity.

1. Introduction

SCOBY is the commonly used acronym for "symbiotic culture of bacteria and yeast," and is formed after the completion of a unique symbiotic fermentation process of acetic acid bacteria (AAB) and yeast to form beverages such as kombucha [1]. The biofilm of cellulose that embraces bacteria and yeast of the SCOBY disc is a by-product of kombucha tea fermentation. Several studies on the kombucha SCOBY are being carried out to exploit all the possibilities of dealing with this cellulose as a suitable raw material in fields of food technology, biomaterial preparation, fashion, textile industries, and environmental biotechnology [39]. To the author's knowledge, this is the first use of the SCOBY disc to induce gold nanoparticles. SCOBY disc of kombucha is composed of yeast and acetic acid bacteria especially, *Gluconacetobacter xylinum* which forms a cellulose pellicle on tea broth [41].

It is produced by fermenting tea using a "symbiotic colony of bacteria and yeast" SCOBY. Actual contributing microbial populations in SCOBY cultures vary, but the yeast component generally includes *Saccharomyces* and other species, and the bacterial component almost always includes *Gluconacetobacter xylinus* to oxidize yeast-produced alcohols to acetic and other acids [2]. The SCOBY disc of kombucha had been used for ages in many countries, especially in Japan, Russia, China, and Eastern Europe as a starter in the fermentation process of tea broth. Nowadays, the yield beverage from the fermentation of tea by SCOBY Kombucha is generally regarded as a universal natural medicament popular and consumed for having a strengthening effect on the human body health [42]. Kombucha SCOBY is described as a "miraculous medicament that cures every condition" [43]. It is supposed to improve vision, purify the body, the strengthen immune system, and decrease the risk of cancer [42].

Gold nanoparticles are of interest mainly due to their stability under atmospheric conditions, resistance to oxidation, and biocompatibility [3, 4]. Therefore, the development of techniques for the synthesis of gold nanoparticles, of well-defined size and shape, is a great challenge. Different chemical methods developed to control the physical properties of the particles for their different applications. Most of these methods are still in the development stage, and problems are often experienced with the stability of the nanoparticle preparations, control of the crystal growth, and aggregation of the particles [5, 6]. There is increasing pressure to develop clean, nontoxic, and environmentally safe technologies. Microbial resistance against heavy metal ions has been exploited for biological metal recovery via the reduction of the metal ions or the formation of metal sulfides [3]. Recently, microorganisms such as fungi and bacteria were shown to be attractive alternative ways to synthesize gold nanoparticles [7]. Metal nanoparticle synthesis depends on the reducing agent, which reduces the state ($Au^{3+} \rightarrow Au^0$)[8]. It is worth mentioning that silver nanoparticles were induced using the SCOBY disc by M. Shanmugavel *et al*. in 2017 [44].

2. Materials and methods:

2.1. SCOBY of kombucha

The SCOBY disc was kindly provided by **Prof. M. Hossam Aboul-Nasr** Fig.1. Then the SCOBY was activated and fermented every 2 weeks to get a new batch of SCOBY.

Fig. 1: (**A**) Label of shipping bag (Poly mailers) from USA. (**B**) SCOBY disc of kombucha

2.2. Growth conditions

The SCOBY disc was grown aerobically in a liquid black tea media. The biomass was harvested after 7 days of growth, followed by extensive washing with deionized water to remove any medium component from the biomass.

2.3. Cell filtrate extract preparation

SCOBY biomass (10 gm fresh weight) was brought in contact with 100 mL of sterilized deionized water for 72 h at 28ºC in an Erlenmeyer flask and agitated in a rotary shaker (120 rpm) in dark condition. After the incubation, the cell-free extract was obtained using Whatman filter paper No.1.

2.4. Chemicals:

2.4.1. Gold chloride solution Preparation

Trihydrated tetrachloroauric acid ($HAuCl_4.3H_2O$) (purchased from Sigma Aldrich) was used for the synthesis of gold nanoparticles by adding 0.0357g of ($HAuCl_4.3H_2O$) to 100 mL sterilized deionized water to produce 1mM aqueous solution.

2.5. Biosynthesis of gold nanoparticles

The SCOBY disc of kombucha was inoculated into the sterile liquid black tea medium and incubated at room temperature for 7 days. Further, the SCOBY was collected, washed, suspended in sterile distilled water (DW), and agitated (120 rpm) at room temperature for 72 h. The supernatant (cell-free extract) collected after centrifugation was used for the synthesis of nanoparticles. An equal volume of 1 mM ($HAuCl_4$) solution was mixed with cell-free extract (CFE) and agitated (120 rpm) in the dark at room temperature. Simultaneously, 1 mM ($HAuCl_4$) solution was maintained as a control under similar conditions. To probe the role of biomolecules (acting as reducing agents) present in the (CFE), one set of experiments was also performed where heat-treated (CFE) was challenged with 1 mM ($HAuCl_4$) solution. The formation of gold nanoparticles was routinely monitored by visual inspection as well as recording the UV-Visible spectra of the reaction mixture [40].

2.6. Characterization of gold nanoparticles:

To determine the characterization of nanoparticles, many techniques are used: The surface area, core size, solubility, particle size distribution, aggregation, zeta potential, adsorption potential, shape, size of the interactive surface, and the intercalation and dispersion of nanoparticles [9].

2.6.1. UV-Vis spectra analysis

Characterization of AuNPs by visual observation for change in color from pale yellow to red-purple considered as the first observation for the gold nanoparticles synthesis and further formation of AuNPs was confirmed by UV-visible spectroscopy for the appearance of characteristic surface plasmon resonance (SPR) band of AuNPs [10]. The biotransformation of ($Au^{3+} \rightarrow Au^0$) was also observed by sampling aliquots (2 mL) of the aqueous solution at different time intervals and measuring the UV-Vis spectra of the solution. The synthesized AuNPs were proven by sampling the reaction mixture at regular terms and the absorption spectra were scanned at the wavelength from 400 to 700 nm using JENWAY 7315 spectrophotometer, UK. Spectroscopic analysis of several weeks-old samples was also carried out to check the stability of the synthesized gold nanoparticles.

2.6.2. Transmission electron microscopy (TEM)

The size and shape of the synthesized AuNPs were determined using a transmission electron microscope (TEM) model JEM100CX11 JEOL (Japan). A 10-fold diluted sample of the synthesized AuNPs was mounted on carbon-coated copper grids and held in a vacuum for the night before being loaded into the specimen holder. The size of the AuNPs was determined at 100KV (0.23 nm resolution), Electron Microscopy Unit, Assiut University, Assiut, Egypt.

2.6.3. (FTIR) spectroscopy analysis

To examine the potential functional groups involved in biosynthesis, the (FTIR) spectrum of the prepared sample was recorded in a Bruker, Alpha-A, Germany in the range of 4000 – 400 cm^{-1} at a resolution of 4 cm^{-1}. Fourier transform infrared spectroscopy (FTIR) was applied for the analysis of the obtained AuNPs [11]**.** Dried sample of the synthesized gold nanoparticles has been dried by using a simply modified method developed by M. B. Aboul Nasr *et al.* [12], where chloroform was mixed with an aqueous sample of gold nanoparticles solution in a ratio of (1: 1) for one hour. The aqueous solution separated from the gold nanoparticles found on the surface of the chloroform was removed by a micropipette and then evaporated chloroform to obtain the dried sample of AuNPs at room temperature.

2.6.4. Particle size analysis

The mean particle size and polydispersity index (PDI) of the nanoparticles were measured using a Zetasizer Nano ZS instrument (Malvern Instruments, Worcestershire, UK) equipped with a backscattered light detector operating at 173°. The Zeta-potential values were measured by laser Doppler anemometry using Malvern Zetasizer Nano series ZS. The sample was diluted in distilled water and measured at 25°C in

triplicates (equilibrium time of 120 s and 15 runs). The sample's volume used for measurements was kept constant.

2.6.5. Zeta potential measurement

The suspension of the synthesized gold nanoparticles was diluted 10 times and the diluted sample was allowed to filter through a 0.22 μm syringe-driven filter unit. The filtered sample of gold nanoparticles was considered to measure the Zeta potential using the same instrument for (DLS).

2.6.6. X-ray diffraction XRD

The crystallinity of samples was evaluated by wide-angle X-ray diffraction (WAXD) analysis using XDL 3000 powder X-ray diffractometer, (Ain Shams University) operated with Cu Kα radiation (λ = 0.15418 nm). Diffraction patterns were recorded over a (2θ). Range of 20-80 in continuous mode. Data were collected with steps of 0.021° (2θ) [13].

2.7. Anticancer activity of gold nanoparticles against HepG2 cell lines:

2.7.1. Cytotoxicity assay

To check the cytotoxic effect of the biosynthesized gold nanoparticles on tumors, the cytotoxic activity of the attained gold nanoparticles based on SCOBY disc was detected (*in vitro*) and considered at one concentration (0.5mM) against human liver cancer cell lines HepG2. The cytotoxic effect of (0.5mM) concentration of AuNPs was determined using 3-(4,5-dimethyl thiazol-2-yl)-2,5-diphenyl- tetrazolium bromide (MTT) assay.

2.7.2. Cell culture

The liver hepatocellular adenocarcinoma HepG2 cell line was obtained from the GIBCO (Grand Island Biological Company), USA. Cells were cultured in RPMI-1640 medium supplemented with 10% fetal bovine serum (FBS), 100 U/mL of penicillin, and 100 μg/mL of streptomycin and were incubated in a humidified atmosphere containing 5% CO_2 and 95 % air at 37°C according to the guide book of the cell line bank.

2.7.3. Cell Viability and AuNPs IC50 Evaluation

Liver cancer cell lines-HepG2 cytotoxicity was determined according to AshaRani *et al.* in which cell plates 96-wells were incubated at 37ºC. The supernatant was decanted after four hours and plates were incubated in the dark for 30 min at 37ºC. The absorbance wavelength 570 nm was read using microplate reader Elx-800-Biotek, and the viability percentage in addition to the IC50 value was determined [14].

3. Results and discussion:

3.1. Biosynthesis of gold nanoparticles:

3.1.1. Visual observation

Our results revealed that the SCOBY supernatant color changed exceptionally from pale yellow to purple color momentarily when the gold chloride was added Fig. 2. The SCOBY disc of kombucha was used to investigate its ability to synthesize AuNPs. The extracellular synthesis of AuNPs using the cell-free extract (CFE) of the SCOBY was verified first visually and the intensity of color increased up in five seconds to dark purple. It is well known that the appearance of purple colours in the reaction mixture indicates the formation of AuNPs [15-17]. Fig. 2 shows conical flasks with a (CFE) of SCOBY disc before and after the reaction with $AuCl_4^-$ ions. The cell-free extract (CFE) has a pale-yellow color before the reaction with the gold ions which changes to purple on completion of the reaction.

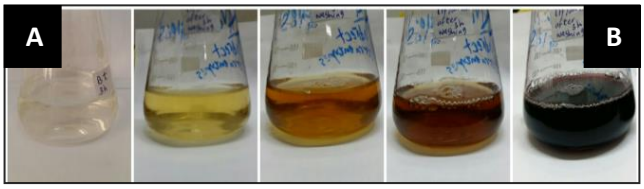

Fig. 2: Shows conical flasks with a cell-free extract (CFE) of kombucha SCOBY disc (A) before and (B) after reaction with $AuCl_4^-$ ions for 5 second. The (CFE) has a pale yellow colour before reaction with the gold ions which changes to purple on completion of the reaction.

3.2. Characterization of the gold nanoparticles:

3.2.1. UV-Vis spectra analysis

Vis-UV absorbance of the gold nanoparticles colloidal solution usually ranges from 510 to 560 and the SCOBY disc supernatant reflected purple color due to their (SPR) of gold nanoparticles resulting in spectroscopic signature shown in Fig. 3. The reduction of chloroauric acid was subjected to spectral analysis using the UV–visible spectrophotometer, which showed an absorbance peak at 530 nm Fig. 3, which was specific for gold nanoparticles reported by V. C. Verma *et al*. [18].

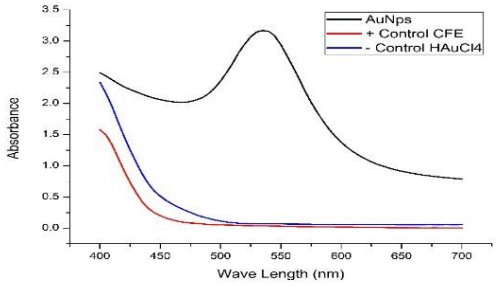

Fig. 3: Shows the UV/Vis spectra recorded for the reaction solution of the (CFE) of black tea-SCOBY disk as positive control, gold chloride as negative control and AuNPs.

Also, M. B. Aboul-Nasr *et al*. reported that the UV-visible spectra of AuNPs solution of *Aspergillus ochraceus* strain AUMC 14355 were observed at 546 nm [19]. Our results agreed with the previous finding of R. Vijayakumar *et al.* using extracts of *Crocus sativus* that showed an absorbance band at 549 nm [20]. Our results agreed with the standard peak resonance wave length confirmed by V. Nachiyar *et al*. [21] at 535 nm. These results reflected a spherical shape of AuNPs. More or less, the same results were obtained by H. Hang & X. yang at 525 nm [22]. That yielded a triangular shape of the gold nanoparticles that located at 540 nm [22].

3.2.2. Transmission electron microscope (TEM) Analysis

The (TEM) showed that gold colloidal solutions produced by the SCOBY disc are variable. They embraced spherical, triangle, and hexagonal shapes with sizes ranging from 14.2 to 39.5 nm Fig. 4.

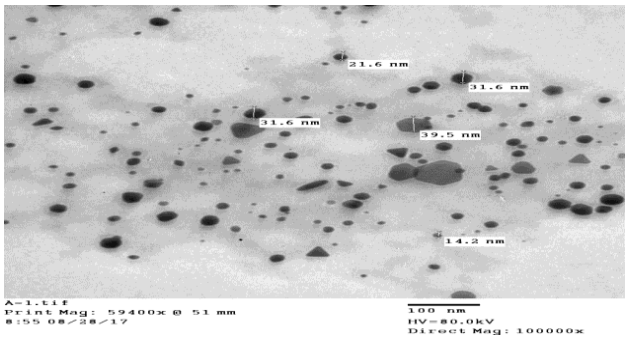

Fig. 4: Transmission electron micrograph of AuNPs synthesized by cell-free extract of kombucha SCOBY disc.

Similar results were obtained with *Candida albicans* where the size of the gold nanoparticles were found to be in the range of 15 – 30 nm [23]. Other studies conducted by V. C. Verma *et al*. [18] also substantiate these results wherein an endophytic fungus *Aspergillus clavatus* was used for the synthesis of gold nanoparticles. The gold nanoparticles AuNPs were stabilized by the proteins that prevent their aggregation; this is in agreement with the UV/vis spectroscopy measurements which showed the gold solutions to be exceptionally stable. The (TEM) results of our AuNPs indicate that it was indeed possible to synthesize gold particles of nanoscale dimensions and tolerable monodispersity by using the kombucha SCOBY disc. The gold nanoparticles synthesised with SCOBY disc were small in size and monodisperse. Similar results were also reported using Sumac extract for synthesizing of AuNPs by H. Shabestarian *et al*. [24].

3.2.3. Dynamic light scattering (DLS) analysis:

3.2.3.1 Particle size

It is important to mention that the average particle size of AuNPs produced in this study was found to be of 61.23 ± 0.416 nm size using a particle size analyzer. Extracellular reduction of the metal ions by SCOBY resulted in the rapid formation of the highly stable gold nanoparticles of 61.23 ± 0.416 nm dimensions. The nanoparticles were not in direct contact within the aggregates, indicating stabilization of the nanoparticles by capping agents. The (DLS) investigation showed AuNPs produced in this work with 0.399 ± 0.019 Polydispersity Index (PDI) value (Table 1). Polydispersity Index (PDI) refers to the distribution of size populations within a sample and the obtained single peaks indicated good quality of the synthesized gold nanoparticles is good Fig. 5.

The AuNPs displayed the polydispersity index (PDI of 0.39) according to some researches, a (PDI) value of 0.1 ‑ 0.25 specifies a narrow size distribution while a (PDI) > 0.5 refers to a broad distribution [25]. Thus, the obtained size distribution for the prepared AuNPs (PDI) value of 0.39 showed a narrow size distribution. The (PDI) of AuNPs synthesized by *A. terreus* was found to be 0.864±0.015 [26].

Table 1 : Average particle size (nm), (PDI), and Zeta potential (mV) of AuNPs reduced with kombocha SCOBY disc.

Formulation	Average particle size (nm)	(PDI)	Zeta-potential (mV)
AuNPs reduced with kombocha SCOBY disc	61.23 ± 0.416	0.399 ± 0.019	-10.2 ± 1.73

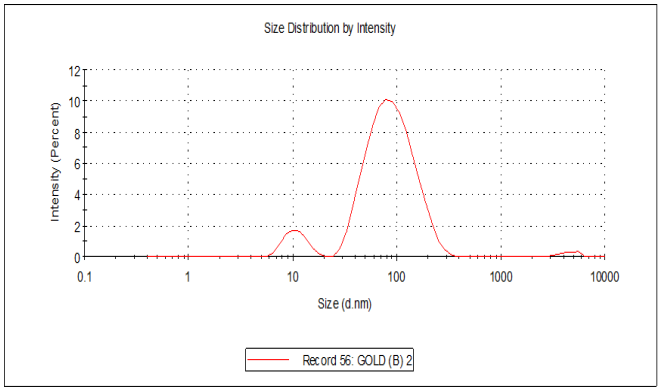

Fig. 5: Particle size distribution curve of SCOBY - AuNPs

3.2.4. Zeta potential measurement

The Zeta potential of suspended AuNPs induced in our lab was measured as shown in (Table 1), to determine the surface charge and stability of the nanoparticles in aqueous dispersion. The surface charge is a main factor generally used to predict a nanoparticle's stability. The stability of nanoparticles in aqueous is strongly correlated to their zeta potential. SCOBY disc-AuNPs formulations were negatively charged -10.2 ± 1.73 mV, indicating their excellent colloidal stability through electrostatic repulsion between them Fig. 6.

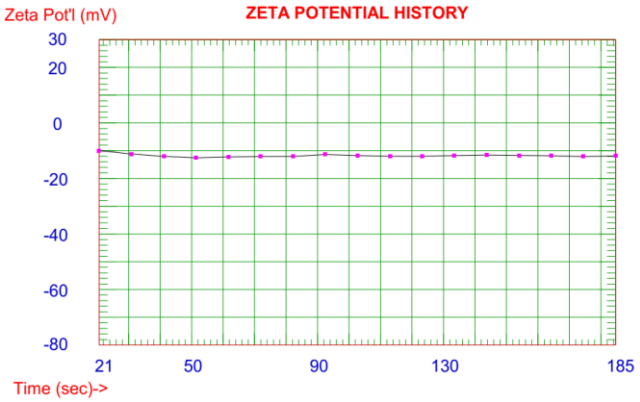

Fig. 6: Zeta potential plot of AuNPs synthesized by SCOBY

Our findings agreed with those of many previous studies where zeta potential (Surface potential) has a direct relation with the stability of a structure when the potential charge is around ±10 to ±30 stability of synthesized nanoparticles was moderate [27]. N. A. El-araby *et al.* showed that the freshly prepared AuNPs formulations produced by *A. terreus, A. ochraceus, A. quadrilineatus, A. fumigatiaffinis* were negatively charged, varying from (-5.54 to -14.89 mV) [26].

3.2.5. X-Ray diffraction XRD analysis

The crystallinity of SCOBY disc-AuNPs was investigated by X-ray diffraction XRD technique, and corresponding XRD patterns were shown in Fig. 7.

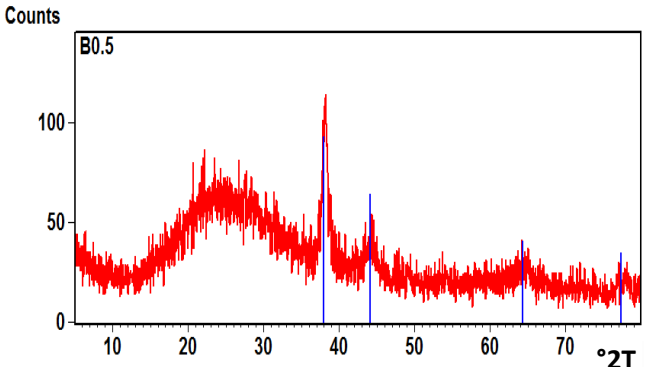

Fig. 7: X-ray diffraction pattern of AuNPs synthesized using SCOBY disc. The Bragg reflections are indexed based on the fcc gold structure.

To prepare the sample in dried form, a simple modified approach was used by extracting AuNPs from the aqueous solution using chloroform. The chloroform extract was separated from the aqueous solution containing AuNPs using a separated funnel and let them dry by air gun [12]. Synthesized SCOBY disc-AuNPs exhibited four distinct peaks at 2θ = 38.1°, 44.8°, 64.5°, and 77.4°. All four peaks corresponded to standard Bragg reflections (111), (200), (220), (311), and orientations of the face center cubic (fcc) lattice of metallic crystalline gold confirmed the presence of gold nanoparticles (Table 2).

Table 2: Peak list of the X-ray diffraction pattern of SCOBY-AuNPs.

Pos. [°2Th.]	Height [cts]	FWHM Left [°2Th.]	d-spacing	Rel. Int. [%]
38.179680	100.00000	0.090000	2.34480	100
44.872060	55.000000	0.090000	2.03980	45.4
64.564400	45.000000	0.090000	1.45236	16.50
77.450070	40.000000	0.090000	1.23305	15.50

These results indicated that the nanoparticles were composed of highly crystalline Au^0 [28]. The intense diffraction at 38.1° peak shows that the preferred growth orientation of zero-valent gold was fixed in (111) direction. This observation suggested that the (111) plane was the predominant orientation of the prepared AuNPs; this refers to molecular-sized solids formed with a repeating 3D pattern of atoms or molecules with an equal distance between each part. This XRD pattern is typical of pure Au nanocrystals. The current results were in agreement with previously published results of gold nanoparticle synthesis using bacteria [29]. In addition, the present findings in this study were supported by the results obtained by J. Sarkar *et al.* who studied the Mycogenesis of gold nanoparticles using a phytopathogen *Alternaria alternata* and their results showed that the diffraction peak corresponding to the (111) phase was the main peak, indicating that (111) was the primary orientation [15].

V. C. Verma *et al.* reported that the Bragg reflections obtained from the AuNPs correspond to the fcc crystalline structure of gold [18]. The XRD pattern exhibited four identical diffraction peaks corresponding to the (111), (200), (220), and (311) appearing at 2θ = 38.2º, 44.5º, 65.6º and 78.6º of metal gold, respectively (International Center for Diffraction Data, ICDD No. 04–0783), indicating that the precipitate was composed of pure crystalline gold. In addition, in the XRD pattern, a very intense Bragg reflection for the (111) lattice was observed, suggesting that the (111) oriented AuNPs were lying flat on the planar surface, while the reflections correspond to (220) and (311) with a lattice spacing of 1.44 and 1.23 A° was specific for the triangular morphology, respectively [18]. It was also notable that the ratio of intensity between the (200) and (111) diffraction peaks for the prepared sample was much lower than the standard (0.042 vs. 0.33), and this rationally decreased as the particle size increased.

3.2.6. Fourier transform infrared spectroscopy (FT-IR)

A simple modified method to overcome hiding an amides group in the case of aqueous solution extract was used by extracting AuNPs using chloroform. The chloroform extract was separated from the aqueous solution containing AuNPs, collected using a separated funnel, and let dry at room temperature [12].

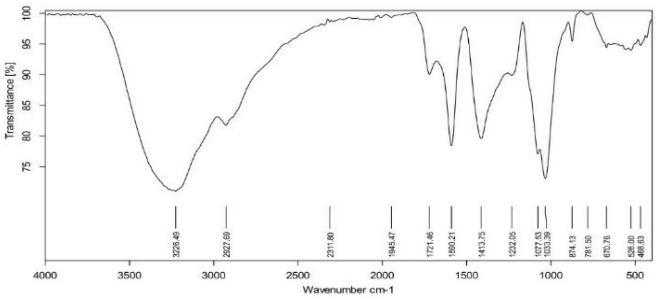

Fig. 8: (FTIR) spectrum of the AuNPs obtained using a cell-free extract of the kombucha black tea- SCOBY disc.

Fig. 8 shows the (FTIR) spectrum of the AuNPs. The sharp bands at 3,226 and 2,927 cm^{-1} suggest the presence of stretching vibrations (N—H) of primary and secondary amines, and aldehydic C—H stretching, respectively. Moreover, this also indicates the possibility of hydroxyl functional groups, which might have arisen from alcohols or phenols present in the

SCOBY extract. On the other hand, their corresponding N—H bending vibration was seen at 1,721 and 1,033 cm^{-1}, respectively. In addition, the weak bands at 1,413 and 1,077 cm^{-1} were assigned to C—N stretching vibrations of aromatic and aliphatic amines. Hence, the presence of amide linkages to hold the amino acid residues of the protein biomolecules, such as tryptophan/tyrosine secreted extracellularly by the SCOBY disc was responsible for the possible stabilization of the synthesized AuNPs. These results suggested the presence of proteins on the surface of Au core particles. Similar results suggested that proteins can bind to Au nanoparticles through free amine groups in the proteins [30]. According to N. A. El-araby *et al*. (FTIR) spectrum of biogenic synthesized gold nanoparticles showed the availability of functional groups. More number of functional groups were present in gold nanoparticles. The peaks were observed at range (3371.10 - 3282.22) cm^{-1} corresponding to (N—H of protein with O—H of water and protein). A long narrow band was seen at the wave number of 2955 cm^{-1} indicating the presence of C—H stretched alkane groups. Strong bands were noted at the range (1701, 1639.95, and 1462.57) representing the C—C stretch (in-ring) of aromatics and N—O symmetric stretch nitro groups, respectively. C—N stretch aromatic amines and C—N stretch aliphatic amines showed at 1246.47 and 1034.01 respectively [26]. (FTIR) the spectrum revealed two peaks at 1635.83 and 1564.68 cm^{-1} that corresponds to the bending vibrations of the amide I and amide II bands of the proteins respectively; while their corresponding stretching vibrations were seen at 3301.49 and 3203.40 cm^{-1} for (N—H of protein with O—H of water and protein) stretching [27].

3.3. Cytotoxicity assay (MTT):

3.3.1. IC50 value

Cytotoxic effect of SCOBY- synthesized AuNPs was performed on liver cancer cell line HepG2 and determined using 3-(4,5-dimethylthiazol-2-yl)-2,5-diphenyltetrazolium bromide (MTT) assay. Recorded data revealed that viability was concentration-dependent, where the viability increases as long as the concentrations of AuNPs decrease till reaching 100% viability at a concentration of 1 µM/mL. Cytotoxicity was assessed by quantitative analysis of damage to the plasma membrane. Our results of (the MTT) assay showed that AuNPs produced by SCOBY disc have a high toxic effect on HepG2 cells with an IC50 value of 176 µM/mL. This induced decreased viability of the liver cancer cell line Fig. 9. Data recorded revealed a significant decrease in IC50 value Fig. 10. Similar to our results H. M. Ebrahim *et al*. found that the half inhibition concentration IC50 following incubation of HepG2 cells with different concentrations of AuNPs for 48 hrs was found to be 176.6 µmol/L [31]. Exposure of HepG2 cells for 48 hrs to increasing levels of AuNPs concentration (50-250 µmol/L) gave rise to a dose-dependent significant decrease in cellular growth, as demonstrated by the significant decrease in (MTT) absorbance at all AuNPs concentrations, compared to untreated HepG2 control. Furthermore, the addition of increasing concentrations of AuNPs in HepG2 cells culture media reduced the percentage of cell viability in a significant dose-dependent manner, where the highest AuNPs dose (250 µM/L) recorded the greatest cytotoxicity on HepG2 cells (68.85%) [31].

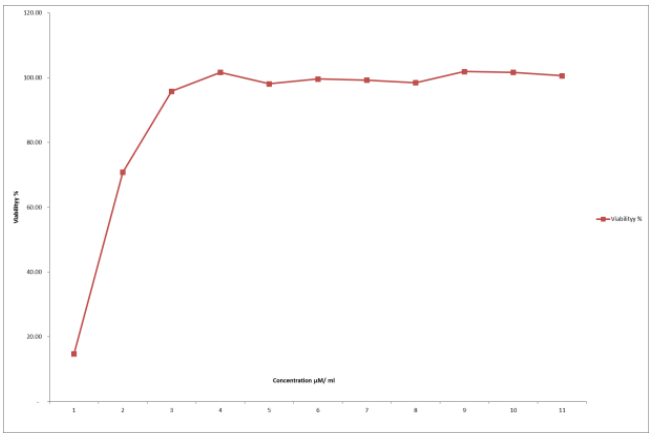

Fig. 9: Evaluation of cytotoxicity of AuNPs produced by SCOBY on liver cancer cell line HepG2 using (MTT) assay.

About potential of gold nanoparticles, they have been used in the treatment of various cancers such as human glioma, colon cancer, lung epithelial cancer, breast carcinoma, uterine cancer, and human lung cancer [32]. It was found that the anticancer of AuNPs is highly dependent on several factors related to its physical properties such as shape, surface coverage, and size. Regarding size, it has been stated that small-sized gold nanoparticles can transfer and remove the cell membrane of tumor cells. In the larger size, the above capability is significantly limited [33]. As shown in the TEM micrograph of our study, gold nanoparticles had a spherical morphology with a size range from 14.2 to 39.8 nm that agrees with those of the size of gold nanoparticles below 50 nm is well suited for killing tumor cell lines *in vivo* and *in vitro* [33]. M. B. Aboul-Nasr *et al*. reported by the (MTT) assay that AuNPs have a high toxic effect on MDAMB-231 cells with IC50 value 32.83 µM/mL for those of *A. ochraceus* AUMC 14355[12]. M. A. Abu-Tahon *et al*. have stated that AuNPs had a strong toxic impact on A549 and HepG2 cells, with IC50 values of 53.5µg/mL and 60.7 µg/mL, respectively. And a moderate cytotoxic impact on MCF7 cells, with an IC50 value of 100µg/mL [34]. The cytotoxic effect of AuNPs is the result of the active physicochemical interaction of gold atoms with the functional groups of intracellular proteins as well as with the nitrogen bases and phosphate groups in DNA, causing cell damage and inhibiting protein synthesis [35-37]. M. E. Selim. & A. A. Hendi stated that the toxic responses of gold nanoparticles to human breast epithelial MCF-7 cells were investigated. Their results demonstrated that exposure of gold nanoparticles to MCF-7 cells causes cytotoxicity. They have also exhibited apoptotic responses of AuNPs in MCF-7 cells. (MTT) assays revealed that the AuNPs exert significant cytotoxicity to MCF-7 cells in a dose-dependent fashion in the concentration range of 25-200 µg/mL [37]. According to the study of Y. J. Lee *et al*., the anticancer activity of biogenic AuNPs against HepG2 cells is shape-dependent. After 24 h of treatment of HepG2 cells with biogenic AuNPs using (MTT) assays, the IC50 value was found at 127.1 µM/mL for nanospheres [38].

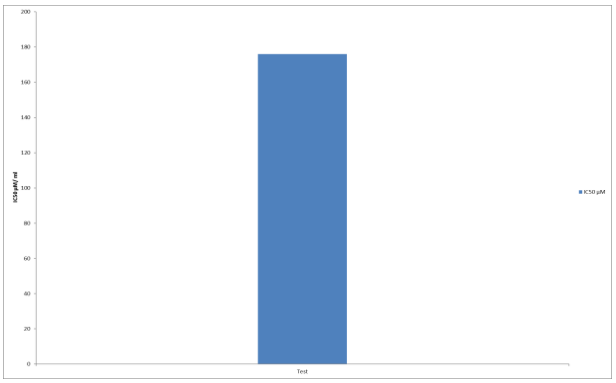

Fig. 10: Evaluation IC50 of AuNPs - SCOBY by (MTT) assay on liver cancer cell line HepG2.

4. Conclusion

SCOBY disc of Kombucha proved to induce highly stable and eco-friendly AuNPs. The in vitro cytotoxicity studies showed promising results of very selective potentiality of these synthesized AuNPs to kill liver cancer cells. This encourages us to recommend their use in liver cancer treatment and further clinical studies must be recommended.

References

[1] S. A. Villarreal-Soto, S. Beaufort, J. Bouajila, J. P. Souchard & P. Taillandier, *Journal of food science*, 83 (2018), 580-588.

[2] R. Jayabalan, R. V.Malbaša, E. S.Lončar, J. S.Vitas & M. Sathishkumar, *Comprehensive reviews in food science and food safety*, 13 (2014), 538-550.

[3] M. Gericke & A. Pinches, *Hydrometallurgy*, 83 (2006), 132-140.

[4] J. Huang, Q. Li, D. Sun, Y. Lu, Y. Su, X. Yang, H. Wang, Y. Wang, W. Shao, N. He, *Nanotechnology*, 18 (2007), 105104.

[5] S.P. Chandran, M. Chaudhary, R. Pasricha, A. Ahmad & M. Sastry, *Biotechnology progress*, 22 (2006), 577-583.

[6] S. S. Shankar, A. Rai, A. Ahmad & M. Sastry, *Journal of colloid and interface science*, 275 (2004), 496-502.

[7] T. Klaus, R. Joerger, E. Olsson, & C.G. Granqvist, *Proceedings of the National Academy of Sciences*, 96 (1999), 13611-13614.

[8] P. Mukherjee, A. Ahmad, D. Mandal, S. Senapati, S. R.Sainkar, M.I. Khan & M. Sastry, *Nano letters*, 1 (2001), 515-519.

[9] V. Bansal, D. Rautaray, A. Bharde, K. Ahire, A. Sanyal, A. Ahmad & M. Sastry, *Journal of Materials Chemistry*, 15 (2005), 2583-2589.

[10] A. R. Shahverdi, S. Minaeian, H. R. Shahverdi, H. Jamalifar & A. A. Nohi, *Process Biochemistry*, 42 (2007), 919-923.

[11] S. Chen & K. Kimura, *Langmuir*, 15 (1999), 1075-1082.

[12] M. B. Aboul-Nasr, S. S. Mohamed & A. A. Yasien, *Journal of Environmental Studies*, 24 (2021), 42-52.

[13] E. Raub & M. Engel, *International Journal of Materials Research*, 39 (1948), 172-177.

[14] P. V. AshaRani, G.L.K. Mun, M. P. Hande & S. Valiyaveettil, *ACS Nano*, 3 (2009), 279–290.

[15] J. Sarkar, S. Ray, D. Chattopadhyay, A. Laskar & K. Acharya, *Bioprocess and Biosystems Engineering*, 35 (2012), 637-643.

[16] S. Balasubramanian, S. M. J. Kala & T. L. Pushparaj, *Journal of Drug Delivery Science and Technology*, 57 (2020), 101620.

[17] P. Rajasekharreddy, P. UshaRani, & B. Sreedhar, *Journal of Nanoparticle Research*, 12 (2010), 1711-1721.

[18] V. C. Verma, S. K. Singh, R. Solanki & S. Prakash, *Nanoscale Res Lett*, 6 (2011), 1-7.

[19] M. B. Aboul-Nasr, S. S. Mohamed & N. A. El-araby, *Sohag Journal for Young Scientific Researcher*, 29 (2021).

[20] R. Vijayakumar, V. Devi, K. Adavallan & D. Saranya, *Physica E: Low-Dimensional Systems and Nanostructures*, 44 (2011), 665-671.

[21] V. Nachiyar, S. Sunkar & P. Prakash, *Der Pharma Chemica*, 7 (2015) 31–38.

[22] H. Huang, & X. Yang, *Colloids and Surfaces A: Physicochemical and Engineering Aspects*, 226 (2003), 77-86.

[23] A. Chauhan, S. Zubair, S. Tufail, A. Sherwani, M. Sajid, S. C. Raman & M. Owais, *International journal of nanomedicine*, 2305 (2011) - 2319.

[24] H. Shabestarian, M. Homayouni-Tabrizi, M. Soltani, F. Namvar, S. Azizi, R. Mohamad & H. Shabestarian, *Materials Research*, 20 (2016) 264-270.

[25] L. K. Limbach, P. Wick, P. Manser, R. N. Grass, A. Bruinink & W.J. Stark, *Environmental science & technology*, 41 (2007) 4158-4163.

[26] N. A. El-araby, M. B. Aboul-Nasr, S. S. Mohamed, *master`s thesis*, University of Sohag, 197 (2021).

[27] A. A. Yasien, M. B. Aboul-Nasr, S. S. Mohamed, *master`s thesis*, University of Sohag, 214 (2021).

[28] N. Vigneshwaran, N. M. Ashtaputre, P. V. Varadarajan, R. P. Nachane, K. M. Paralikar & R. H. Balasubramanya, *Materials letters*, 61 (2007) 1413-1418.

[29] M. I. Husseiny, M. Abd El-Aziz, Y. Badr & M. A. Mahmoud, *Spectrochimica Acta Part A: Molecular and Biomolecular Spectroscopy*, 67 (2007) 1003-1006.

[30] A. Gole, C. Dash, V. Ramakrishnan, S. R. Sainkar, A. B. Mandale, M. Rao & M. Sastry, *Langmuir*, 17 (2001) 1674-1679.

[31] H. M. Ebrahim, E. El-Rouby, M. E. Morsy, M. M. Said & M. K. Ezz, *Asian Pacific journal of cancer prevention: APJCP*, 20 (2019) 3369.

[32] L. Dou, X. Zhang, M. M. Zangeneh & Y. Zhang, *Bioorganic chemistry*, 106 (2021) 104468.

[33] F. Namvar, H. S. Rahman, R. Mohamad, J. Baharara, M. Mahdavi, E. Amini & S. K. Yeap, *International Journal of Nanomedicine*, 9 (2014) 2479.

[34] M. A. Abu-Tahon, M. Ghareib & W. E. Abdallah, *Process Biochemistry*, 95 (2020) 1-11.

[35] R. Manikandan, B. Manikandan, T. Raman, K. Arunagirinathan, N. M. Prabhu, M. J. Basu & A. Munusamy, *Molecular and Biomolecular Spectroscopy*, 138 (2015) 120-129.

[36] Y. P. Blagoi, V.N. Zozulya, I. M. Voloshin, V. L. Makitruk, A. S. Shalamay & A. S.

Shcherbakova,. *Biopolymers and Cell*, 13 (1997) 22-29.
[37] M. E. Selim & A. A. Hendi, *Asian Pacific Journal of Cancer Prevention*, 13 (2012) 1617-1620.
[38] Y. J. Lee, E.Y. Ahn & Y. Park, *Nanoscale research letters*, 14 (2019) 1-14.

[39] D. Laavanya, S. Shirkole & P. Balasubramanian, *Journal of Cleaner Production*, 295 (2021) 126454.
[40] Z. Sadowski, *Silver nanoparticles*, 22 (2010) 257-277.
[41] D. Dutta & R. Gachhui, *International Journal of Systematic and Evolutionary Microbiology*, 57 (2007), 353-357.
[42] K. Yapar, K. Cavusoglu, E. Oruc & E. Yalcin, *Journal of Environmental Biology*, 31 (2010), 615.
[43] D. Kaczmarczyk & S. Lochyński, *Polish Journal of Natural Sciences*, 29 (2014), 381-392
[44] M. Shanmugavel, N. Nandhini, B. Supriya, S. Vasantharaj, S. Inbasekaran, A. Gnanamani, *International Journal on Applied Bioengineering*.11 (2017), 22–26.